Published in final edited form as:
Exp Eye Res. 2012 January ; 94(1): 150–156. doi:10.1016/j.exer.2011.11.022.

Low humidity environmental challenge causes barrier disruption and cornification of the mouse corneal epithelium in mice via a c-jun N-terminal kinase 2 (JNK2) pathway

FSA Pelegrino[1], **SC Pflugfelder**[1], and **CS De Paiva**[1]

[1]Ocular Surface Center, Department of Ophthalmology, Cullen Eye Institute, Baylor College of Medicine, Houston, Texas

Abstract

Patients with tear dysfunction often experience increased irritation symptoms when subjected to drafty and/or low humidity environmental conditions. The purpose of this study was to investigate the effects of low humidity stress (LHS) on corneal barrier function and expression of cornified envelope (CE) precursor proteins in the epithelium of C57BL/6 and c-jun N-terminal kinase 2 (JNK2) knockout (KO) mice. LHS was induced in both strains by exposure to an air draft for 15 (LHS15D) or 30 days (LHS30D) at a relative humidity <30%RH. Nonstressed (NS) mice were used as controls. Oregon-green-dextran uptake was used to measure corneal barrier function. Levels of small proline rich protein (SPRR)-2, involucrin, occludin, and MMP-9 were evaluated by immunofluorescent staining in cornea sections. Wholemount corneas immunostained for occludin were used to measure mean apical cell area. Gelatinase activity was evaluated by *in situ* zymography. Expression of MMP, CE and inflammatory cytokine genes was evaluated by q-PCR. C57BL/6 mice exposed to LHS15D showed corneal barrier dysfunction, decreased apical corneal epithelial cell area, higher MMP-9 expression and gelatinase activity and increased involucrin and SPRR-2 immunoreactivity in the corneal epithelium compared to NS mice. JNK2KO mice were resistant to LHS-induced corneal barrier disruption. MMP-3,-9,-13, IL-1α, IL-1β, involucrin and SPRR-2a RNA transcripts were significantly increased in C57BL/6 mice at LHS15D, while no change was noted in JNK2KO mice. LHS is capable of altering corneal barrier function, promoting pathologic alteration of the TJ complex and stimulating production of CE proteins by the corneal epithelium. Activation of the JNK2 signaling pathway contributes to corneal epithelial barrier disruption in LHS.

Keywords

low humidity stress; corneal barrier function; cornified envelop proteins; JNK2 pathway

Corresponding author: Cintia S. De Paiva, M.D., Cullen Eye Institute, Baylor College of Medicine, 6565 Fannin Street, NC 205, Houston, TX 77030; cintiadp@bcm.tmc.edu.

Competing interest: none

1. Introduction

Tear dysfunction is one of the most common medical problems that affects 6 to 44 million people in the United States based on reported prevalence figures of 2 to 14.4% (Moss, Klein and Klein, 2004;Schaumberg, Sullivan, Buring et al, 2003;Schein, Munoz, Tielsch et al, 1997). Patients with tear dysfunction often experience increased irritation symptoms when subjected to drafty and/or low humidity environmental conditions (Guo, Lu, Chen et al, 2010;Gupta, Prasad, Himashree et al, 2008;Lu, Chen, Liu et al, 2008). Many dry eye patients live and work in controlled low humidity environmental conditions, and the irritation they experience from this environment may decrease their productivity and quality of life (Su, Wang, Tai et al, 2009). Australian pilots reported a marked association of dry eye symptoms during flight, as opposed at other times (McCarty and McCarty, 2000).

There are several animal models of dry eye currently in use throughout the world. They are either spontaneous or induced. Several spontaneous models with lymphocytic infiltration of the lacrimal and salivary glands and ocular surface inflammation mimic Sjögren's syndrome to a certain extent. We had developed and characterized an inducible dry eye model where mice are subjected to cholinergic blockade and chronically exposed to a drafty environment where we observed disruption of corneal barrier function, increased production of pro-inflammatory cytokines and metalloproteinases (MMP), activation of mitogen-activated protein kinase (MAPK) intracellular pathways and production of cornified envelope (CE) protein precursors (Corrales, Stern, de Paiva et al, 2006;de Paiva, Pangelinan, Chang et al, 2009;Luo, Li, Corrales et al, 2005;Pflugfelder, Farley, Luo et al, 2005).

The purpose of this study was to investigate if subjecting mice to a desiccating environment without pharmacological inhibition of lacrimal gland would be sufficient to alter corneal barrier function secretion and gene expression in the mouse corneal epithelium and to investigate the role of JNK2 pathway in this process.

2. Material and Methods

2.1. Low humidity stress model

This research protocol was approved by the Baylor College of Medicine Center for Comparative Medicine, and it conformed to the standards in the ARVO Statement for the use of animals in Ophthalmic and Vision Research.

Low humidity stress (LHS) was induced in C57BL/6 mice (n=60), and JNK2 knockout mice (KO) aged 6-8 weeks in a C57BL/6 background (n=40; B6.129S2-*Mapk9tm1Flv/J*, Jackson Laboratories, Bar Harbor, ME) by exposure to a drafty low humidity (<30% ambient humidity; mean ± SD of 25.42±3.38%RH) environment for 7, 15 or 30 days (LH7D, LH15D and LH30D, respectively). Nonstressed (NS) control mice were kept in a separate room with >45% relative humidity (ambient humidity, mean ± SD 55.25±7.37%RH). The mean temperature in the low humidity room was 22.08±0.85 °C vs. 21.78±0.57 °C in the vivarium.

2.2. Histology

Eyes and ocular anexae (n=3 per group) were surgically excised, fixed in 10% formalin, and paraffin embedded or embedded in optimal cutting temperature (OCT compound; VWR, Suwanee, Georgia) and flash frozen in liquid nitrogen. Sagittal 8μm tissue sections were cut and placed on glass slides that were stored at -80 °C (cryosections) or at room temperature (paraffin-embedded) until they were used. Sections were stained with heamatoxylin and eosin (H&E) and were examined and photographed with a microscope equipped with a digital camera (Eclipse E400 with a DS-Fi1; Nikon, Melville, NY).

2.3. Corneal Permeability

Corneal epithelial permeability to 70kDaOregon green dextran (OGD; Invitrogen, Eugene, Oregon) was assessed in C57BL/6 and JNK2KO mice as previously published (de Paiva, Pangelinan, Chang et al, 2009). The severity of corneal OGD staining was graded in digital images in the 2.0-mm central corneal zone of eye by 2 masked observers using NIS Elements software (Nikon, Melville, NY). The mean fluorescence intensity was averaged within each group.

2.4. Occludin Laser Scanning Confocal Immunofluorescent Microscopy

Immunofluorescent staining was performed using polyclonal antibody to immunolocalize occludin protein (1:50, Zymed, Carlsbad, CA) in situ in whole mount corneas using propidium iodide as counterstaining as previously described (Beardsley, de Paiva, Power et al, 2008). Digital images were analyzed using the NIS Elements Software (Nikon). Mean corneal epithelial cell area was measured by outlining 8-10 cells per field per digital image, and the mean peripheral circumferential cell measurement was calculated and averaged within the group.

2.5. Immunofluorescent Staining

Immunofluorescent staining was performed with polyclonal goat antibody to involucrin (1:20; Santa Cruz Biotechnology, Santa Cruz, CA), and SPRR-2 (1:100, rabbit neat serum; Alexis Biochemicals, San Diego, CA) and polyclonal rabbit antibody to metalloproteinase 9 (1:100, Chemicon-Millipore, Billerica, Massachusetts) using appropriate Alexa-Fluor 488 conjugated IgG secondary antibodies and propidium iodide as counterstaining as previously described (de Paiva, Pangelinan, Chang et al, 2009). Digital images were analyzed using the NIS Elements Software (Nikon) Fluorescent intensity was measured by circumscribing the corneal epithelium of each section and the results within each group were averaged.

2.6. In situ zymography assay

In situ zymography was performed to localize gelatinase activity in corneal cryosections because fluorescence is localized to sites of net gelatinolytic activity, using a previous reported method and using propidium iodide as counterstaining (de Paiva, Pangelinan, Chang et al, 2009). Areas of gelatinolytic activity were viewed with a Nikon Eclipse E400 fluorescent microscope and images were captured by a digital camera (Eclipse E400 with DS–F1; Nikon, Melville, NY). Mean fluorescent intensity was measured by NIS Elements software circumscribing the corneal epithelium of each section and the results within each group were averaged.

2.7. RNA isolation and quantitative real-time PCR

Cornea epithelium from C57BL/6 (n=5/time point), and JNK2KO (n=5/time point) mice was scrapped with a scalpel and total RNA was extracted using a Pico Pure RNA isolation® Kit (Arcturus, Applied Biosystems, Foster City, CA) according to the manufacturer's instructions, quantified by a NanoDrop® ND-1000 Spectrophotometer (Thermo scientific, Wilmington, DE) and stored at -80°C. One sample consisted of pooled eyes of the same animal. Samples were treated with DNase to eliminate genomic DNA contamination, according to the manufacturer's instructions (Qiagen, Valencia, CA). First-strand cDNA was synthesized with random hexamers by M-MuLV reverse transcription (Ready-To-Go You-Prime First-Strand Beads; GE Healthcare, Inc., Arlington Heights, NJ), as previously described (de Paiva, Pangelinan, Chang et al, 2009).

Quantitative real-time PCR was performed with specific MGB probes (Table 1; Taqman; Applied Biosystems, Inc., Foster City, CA) and PCR master mix (Taqman Gene Expression

Master Mix), in a commercial thermocycling system (StepOnePlus™ Real-Time PCR System, Applied Biosystems), according to the manufacturer's recommendations. The results of quantitative PCR were analyzed by the comparative C_T method where target change = $2^{-}\Delta\Delta^{C}{}_{T}$ using GAPDH as an endogenous reference. The mean C_T of relative mRNA level in the non-stressed control group of each strain was used as the calibrator. A nontemplate control and total RNA without retrotranscription were included in all the experiments to evaluate PCR and DNA contamination of the reagents.

2.8. Statistical analysis

One-way ANOVA was used to determine overall statistical significance followed by a two-tailed T-test for individual differences in NS, LH treated groups. A $p \leq 0.05$ was considered statistically significant. These tests were performed using GraphPad Prism 5.0 software (GraphPad Software Incorporation, San Diego, CA).

3. Results

3.1. Low humidity and apical corneal permeability barrier

We compared the morphology of corneas of nonstressed control mice housed in an environment with >50% relative humidity (Figure 1) with those of mice subjected to a low humidity environment (<30%RH) for LH15D and LH30D. In NS mice, we observed a stratified corneal epithelium four to five layers thick with a well defined cuboidal layer. The epithelial cells flattened as they differentiated and moved towards the apical layer (Figure 1). In contrast, the corneal epithelium of mice exposed to a LH environment was thinner than control mice and the cells were less homogeneous in cell size. Desquamation of apical corneal cells was easily observed in LH15D and LH30D corneas (Figure 1). Our results are consistent with those of Chen and colleague who reported similar alterations of corneal epithelial morphology when animals were subjected to a low humidity environment without a fan (Chen, Zhang, Zhang et al, 2008).

Disruption of corneal barrier is a hallmark of human dry eye disease. In humans, corneal permeability is routinely assessed with the small 376 MW fluorescent molecule, sodium fluorescein. Our previous studies showed that in mice, fluorescein diffuses rather rapidly into the stroma, leading to poor discrimination of individual fluorescent dots. In the present study, we used our previously published technique that uses the high MW fluorescent molecule OGD (70kDa) to assess corneal epithelial permeability. Minimal scattered punctate staining or no staining with OGD was observed in the corneas of control mice and mice subjected to 7 days of LHS. Uptake of OGD significantly increased after 15D and 30D of LHS ($p<0.001$ and $p<0.001$ respectively, Figure 2), and punctate and confluent dye staining was observed. Because there was no alteration of the corneal barrier function at 7 days of LHS, we opted to drop this time point for the remaining of our studies.

3.2. Expression of the tight junction protein occludin

Barrier function is maintained in the normal cornea by TJ in the differentiated apical corneal epithelial cells. We have previously reported that in areas of apical desquamation, the remaining subapical cells stained by occludin have a smaller area per cell (Beardsley, de Paiva, Power et al, 2008). Using this same technique, we measured individual apical cell area in whole corneas stained for occludin in each group. In control mice, strong intercellular occludin staining was observed in the apical corneal epithelial layers and occasional detaching apical epithelial cells were observed. In LH15D and LH30D whole mount corneas, detaching and rolled cells and holes where the cells had detached from the apical corneal epithelium were easily observed (Figure 3A). We observed that LH15D and LH30D corneas had a significantly smaller mean epithelial cell area compared to NS

corneas ($p<0.0001$), indicating that the apical cell layer observed in these corneas is comprised of smaller previously subapical cells.

3.3. Immunostaining of MMP-9 and cornified envelope precursors by the cornea epithelium

The expression of MMP-9 and gelatinolytic activity was investigated in cornea sections. Intensity of MMP-9 immunostaining and gelatinase activity in the corneal epithelium peaked at LH15D, and returned to baseline levels at LH30D (Figure 3B-E).

Because we have previously observed increased production of CE precursors by the corneal epithelium of eyes exposed to experimental desiccating stress, we performed immunostaining for two CE protein precursors in corneas of mice subjected to LHS. We observed that expression of SPRR-2 and involucrin was significantly elevated in the cornea epithelium of mice subjected to LHS for 15 days, compared to NS mice ($p<0.001$).

3.4. Gelatinase activity, inflammatory cytokine and cornified envelope precursor gene expression analysis

Because we have previously reported that desiccating stress is capable of increasing MMPs and inflammatory cytokines (Corrales, Stern, de Paiva et al, 2006;de Paiva, Pangelinan, Chang et al, 2009;Pflugfelder, Farley, Luo et al, 2005) we then asked if a LHS would be capable of inducing similar changes in the corneal epithelium. The levels of MMPs, inflammatory cytokines (IL-1α, IL-1β), and cornified envelope precursors (SPRR-2a and involucrin) measured by quantitative PCR are presented in Figure 4. Relative levels of MMP-3,-9,-13, IL-1α and IL-1β mRNA transcripts significantly increased in LH15D compared to baseline in C57BL/6 mice. MMP-9 and IL-1β remained elevated in LH30D corneas, while MMP-3,-13 and IL-1α mRNA transcripts decreased at LH30D, but were still significantly elevated compared to NS control corneas. A significant progressive increase in SPRR-2a and involucrin mRNA transcripts were observed in LH15D and LH30D.

3.5 Low humidity in JNK2KO mice

We previously shown that the stress kinases JNK1 and 2 are activated in an experimental model of dry eye created with systemic scopolamine administration and exposure to a dry drafty environment (de Paiva, Corrales, Villarreal et al, 2006a;Luo, Li, Corrales et al, 2005). Furthermore, JNK2 activation promoted corneal barrier disruption by increasing production of MMPs and CE proteins (de Paiva, Pangelinan, Chang et al, 2009). Therefore, we investigated if the JNK2 pathway was involved in the corneal pathology observed in the LHs. In contrast to C57BL/6 mice, JNK2KO had preserved corneal barrier function following LH stress for 15 or 30 days (Figure 2).

Next, we investigated by qPCR if the protection against of corneal barrier disruption in JNK2KO was associated with failure to upregulate production of upregulation of MMPs and inflammatory cytokines. JNK2KO failed to upregulate expression of MMPs, IL-1α, IL-1β, SPRR-2a and involucrin in the corneal epithelium after exposure to a low humidity stress environment (Figure 4).

4. Discussion

Our results indicate that exposure to a drafty low humidity environment stimulated production of MMPs via a JNK2 mediated pathway that resulted in disruption of corneal epithelial barrier function. This type of corneal response was observed in our previously published studies using a mouse dry eye model that used a systemic pharmacological blockade (de Paiva, Pangelinan, Chang et al, 2009) while the present model uses solely LH environmental stress to induce changes.

We evaluated corneal permeability to the fluorescent marker OGD in two mouse strains (C57BL/6 and JNK2KO) before and after LHS for up to 30 days. The two strains had low uptake of OGD by the corneal epithelium at baseline; however, LH15D caused significant corneal barrier disruption in C57BL/6, but not in the JNK2KO strain. An altered corneal epithelial barrier is identified clinically by staining the cornea with fluorescein dye and it has been used as an efficacy parameter in dry eye clinical trials (Pflugfelder, Maskin, Anderson et al, 2004). Corneal epithelial permeability to fluorescein dye in patients with untreated dry eye was reported to be 2.7 to 3 times greater than in eyes with normal tear function (Gobbels and Spitznas, 1992).

Our results showed that LHS increased the level and activity of MMP-9 in corneas of C57BL/6 mice. We have previously reported that MMPs are implicated in desiccation-induced disruption of corneal barrier function, through cleavage of tight junction proteins, such as occludin and ZO-1 (de Paiva, Corrales, Villarreal et al, 2006b;Pflugfelder, Farley, Luo et al, 2005). In human dry eye patients, MMP-9 activity in tears showed strong correlation with the severity of symptoms and corneal fluorescein staining scores (Chotikavanich, de Paiva, Li et al, 2009).

In addition to MMP-9, we also observed increased expression of MMP-3 and -13, IL-1α and 1β and CE early precursors (SPRR-2 and involucrin) in the corneal epithelium. These findings were accompanied by reduced immunostaining of junctional occludin in the apical corneal epithelium, loss of cell-cell adhesion and increased apical cell desquamation. Mircheff and colleagues have found recently that exposure to adverse environmental conditions can alter cytokine production in the rabbit lacrimal glands (Mircheff, Wang, Thomas et al, 2011).

We demonstrated that the corneas of JNK2KO mice were resistant to low humidity stress. In contrast to C57BL/6 mice, the levels of MMP-9, involucrin and SPRR2a transcripts did not increase in response to LHS in the JNK2KO (Figure 4). JNK pathway has been reported to stimulate production of CE precursor proteins, such as involucrin in the corneal epithelium (Adhikary, Crish, Lass et al, 2004). Activation of MAPK pathways by low humidity and hyperosmolar stress of dry eye have been reported as a major contributor to the observed corneal epithelial pathology in dry eye (Li, Chen, Song et al, 2004;Li, Luo, Chen et al, 2006;Luo, Li, Doshi et al, 2004). We have previously reported that our desiccating stress model of dry eye activates MAPK signaling pathways in the ocular surface epithelia, increases production of the proinflammatory cytokine, IL-1 and stimulates production and activation of MMP-9 (Luo, Li, Doshi et al, 2004). Interestingly, Luo and colleagues showed that JNK activation was observed as early as 4 hours after initiation of desiccating stress and the phosphorylated isoform remained elevated throughout the exposure to desiccation.

In our previously described dry eye model that utilizes cholinergic pharmacological blockade of lacrimal gland secretion, an air draft and low humidity, we observed disruption of corneal barrier function after 5 days of exposure and return to baseline levels at 10 days (Corrales, Villarreal, Farley et al, 2007;de Paiva, Corrales, Villarreal et al, 2006a). In the current study, we observed that exposure to a low humidity alone is capable of inducing corneal changes similar to those seen in the previously reported dry eye model using systemic cholinergic blockade (de Paiva, Pangelinan, Chang et al, 2009); however, it takes longer to achieve comparable levels of corneal barrier disruption (15 days), and spontaneous improvement and return of corneal OGD permeability baseline levels was observed at 30 days. The rate of corneal barrier disruption is different between the two models, but the mechanism responsible for the barrier disruption appears to be similar: activation of JNK2 MAPK, upregulation of MMPs, inflammatory cytokines, and increased expression of CE precursors.

Our findings suggest that human exposure to ambient or artificially created low humidity environment is capable of disrupting corneal barrier function. Indeed a higher prevalence of dry eye symptoms has been reported by workers in clean rooms with a relative humidity of 55% (Su, Wang, Tai et al, 2009). Furthermore, many people experience eye irritation and transient blurred vision after long air flights where air plane cabin humidity is often lower than 20% (McCarty and McCarty, 2000). Therapeutic strategies to prevent or minimize activation of JNK2 signaling pathway may prove to minimize the desiccation response and improve ocular tolerance to low humidity environment.

Acknowledgments

Support: Supported by EY11915 (SCP), NIH Core Grant P30-EY002520, Research to Prevent Blindness, the Oshman Foundation, William Stamps Farish Fund and the Hamill Foundation.

Reference List

Adhikary G, Crish J, Lass J, Eckert RL. Regulation of involucrin expression in normal human corneal epithelial cells: a role for activator protein one. Invest Ophthalmol Vis Sci. 2004; 45:1080–7. [PubMed: 15037572]

Beardsley RM, de Paiva CS, Power DF, Pflugfelder SC. The protease inhibitor doxycycline preserves apical corneal epithelial integrity during desiccating stress. Cornea. 2008; 27(8):935–40. [PubMed: 18724157]

Chen W, Zhang X, Zhang J, Chen J, Wang S, Wang Q, Qu J. A murine model of dry eye induced by an intelligently controlled environmental system. Invest Ophthalmol Vis Sci. 2008; 49:1386–91. [PubMed: 18385054]

Chotikavanich S, de Paiva CS, Li dQ, Chen JJ, Bian F, Farley WJ, Pflugfelder SC. Production and activity of matrix metalloproteinase-9 on the ocular surface increase in dysfunctional tear syndrome. Invest Ophthalmol Vis Sci. 2009; 50:3203–9. [PubMed: 19255163]

Corrales RM, Stern ME, de Paiva CS, Welch J, Li DQ, Pflugfelder SC. Desiccating stress stimulates expression of matrix metalloproteinases by the corneal epithelium. Invest Ophthalmol Vis Sci. 2006; 47:3293–302. [PubMed: 16877394]

Corrales RM, Villarreal A, Farley W, Stern ME, Li DQ, Pflugfelder SC. Strain-related cytokine profiles on the murine ocular surface in response to desiccating stress. Cornea. 2007; 26:579–84. [PubMed: 17525655]

de Paiva CS, Corrales RM, Villarreal AL, Farley W, Li DQ, Stern ME, Pflugfelder SC. Apical corneal barrier disruption in experimental murine dry eye is abrogated by methylprednisolone and doxycycline. Invest Ophthalmol Vis Sci. 2006a; 47:2847–56. [PubMed: 16799024]

de Paiva CS, Corrales RM, Villarreal AL, Farley WJ, Li DQ, Stern ME, Pflugfelder SC. Corticosteroid and doxycycline suppress MMP-9 and inflammatory cytokine expression, MAPK activation in the corneal epithelium in experimental dry eye. Exp Eye Res. 2006b; 83:526–35. [PubMed: 16643899]

de Paiva CS, Pangelinan SB, Chang E, Yoon KC, Farley WJ, Li DQ, Pflugfelder SC. Essential role for c-Jun N-terminal kinase 2 in corneal epithelial response to desiccating stress. Arch Ophthalmol. 2009; 127:1625–31. [PubMed: 20008718]

Gobbels M, Spitznas M. Corneal epithelial permeability of dry eyes before and after treatment with artificial tears. Ophthalmology. 1992; 99:873–8. [PubMed: 1630776]

Guo B, Lu P, Chen X, Zhang W, Chen R. Prevalence of dry eye disease in Mongolians at high altitude in China: the Henan eye study. Ophthalmic Epidemiol. 2010; 17:234–41. [PubMed: 20642346]

Gupta N, Prasad I, Himashree G, D'Souza P. Prevalence of dry eye at high altitude: a case controlled comparative study. High Alt Med Biol. 2008; 9:327–34. [PubMed: 19115918]

Li DQ, Chen Z, Song XJ, Luo L, Pflugfelder SC. Stimulation of matrix metalloproteinases by hyperosmolarity via a JNK pathway in human corneal epithelial cells. Invest Ophthalmol Vis Sci. 2004; 45:4302–11. [PubMed: 15557436]

Li DQ, Luo L, Chen Z, Kim HS, Song XJ, Pflugfelder SC. JNK and ERK MAP kinases mediate induction of IL-1beta, TNF-alpha and IL-8 following hyperosmolar stress in human limbal epithelial cells. Exp Eye Res. 2006; 82:588–96. [PubMed: 16202406]

Lu P, Chen X, Liu X, Yu L, Kang Y, Xie Q, Ke L, Wei X. Dry eye syndrome in elderly Tibetans at high altitude: a population-based study in China. Cornea. 2008; 27:545–51. [PubMed: 18520503]

Luo L, Li DQ, Corrales RM, Pflugfelder SC. Hyperosmolar saline is a proinflammatory stress on the mouse ocular surface. Eye & Contact Lens. 2005; 31(5):186–93. [PubMed: 16163009]

Luo L, Li DQ, Doshi A, Farley W, Corrales RM, Pflugfelder SC. Experimental dry eye stimulates production of inflammatory cytokines and MMP-9 and activates MAPK signaling pathways on the ocular surface. Invest Ophthalmol Vis Sci. 2004; 45:4293–301. [PubMed: 15557435]

McCarty DJ, McCarty CA. Survey of dry eye symptoms in Australian pilots. Clin Experiment Ophthalmol. 2000; 28:169–71. [PubMed: 10981789]

Mircheff AK, Wang Y, Thomas PB, Nakamura T, Samant D, Trousdale MD, Warren DW, Ding C, Schechter JE. Systematic variations in immune response-related gene transcript abundance suggest new questions about environmental influences on lacrimal gland immunoregulation. Curr Eye Res. 2011; 36:285–94. [PubMed: 21405952]

Moss SE, Klein R, Klein BE. Incidence of dry eye in an older population. Arch Ophthalmol. 2004; 122:369–73. [PubMed: 15006852]

Pflugfelder SC, Farley W, Luo L, Chen LZ, de Paiva CS, Olmos LC, Li DQ, Fini ME. Matrix metalloproteinase-9 knockout confers resistance to corneal epithelial barrier disruption in experimental dry eye. Am J Pathol. 2005; 166:61–71. [PubMed: 15632000]

Pflugfelder SC, Maskin SL, Anderson B, Chodosh J, Holland EJ, de Paiva CS, Bartels SP, Micuda T, Proskin HM, Vogel R. A randomized, double-masked, placebo-controlled, multicenter comparison of loteprednol etabonate ophthalmic suspension, 0.5%, and placebo for treatment of keratoconjunctivitis sicca in patients with delayed tear clearance. Am J Ophthalmol. 2004; 138:444–57. [PubMed: 15364229]

Schaumberg DA, Sullivan DA, Buring JE, Dana MR. Prevalence of dry eye syndrome among US women. Am J Ophthalmol. 2003; 136:318–26. [PubMed: 12888056]

Schein OD, Munoz B, Tielsch JM, Bandeen-Roche K, West S. Prevalence of dry eye among the elderly. Am J Ophthalmol. 1997; 124:723–8. [PubMed: 9402817]

Su SB, Wang BJ, Tai C, Chang HF, Guo HR. Higher prevalence of dry symptoms in skin, eyes, nose and throat among workers in clean rooms with moderate humidity. J Occup Health. 2009; 51:364–9. [PubMed: 19542676]

Highlights

- We describe a model where mice are exposed to low humidity environmental stress.
- Low humidity stress induces corneal barrier dysfunction, including tight junction dirsuption.
- Low humidity stress increases cornified envelope precursors and activation of JNK2 pathway.

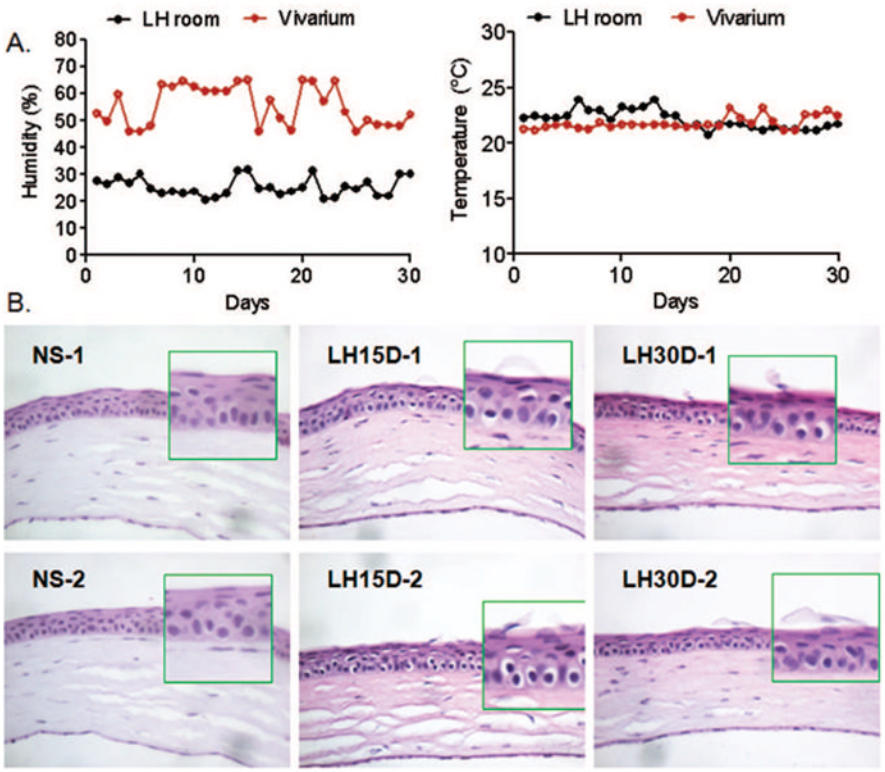

Figure 1.

A. Mean relative humidity (%) and temperature (°C) rec ordings in the Low humidity room (LH) and vivarium throughout the experiment.

B. Representative H&E staining of corneas cryosections of C57BL/6 mice subjected to low humidity stress for 15 and 30 days (LH15D and 30D, respectively). Note desquamation of apical corneal epithelial cells at LH15D and 30D while control eye (nonstressed, NS) showed normal corneal architecture. Original magnification 10X. Insets indicate high magnification of left area immediately adjacent to inset.

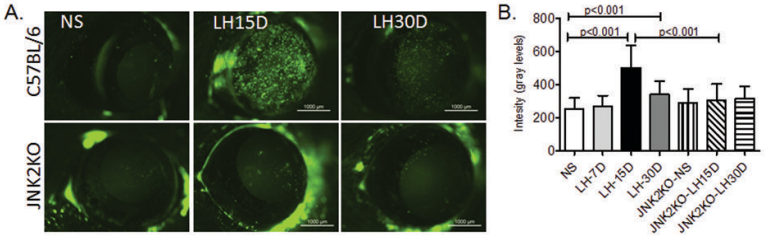

Figure 2. Corneal epithelial permeability of the two strains of mice

A. Representative digital images of corneas of C57BL/6 and JNK2KO mice, nonstressed (NS) and subjected to low humidity stress for 15 (LH15D) or 30 days (LH30D) which were used to generate Oregon green dextran-488 intensity levels shown in **B**.

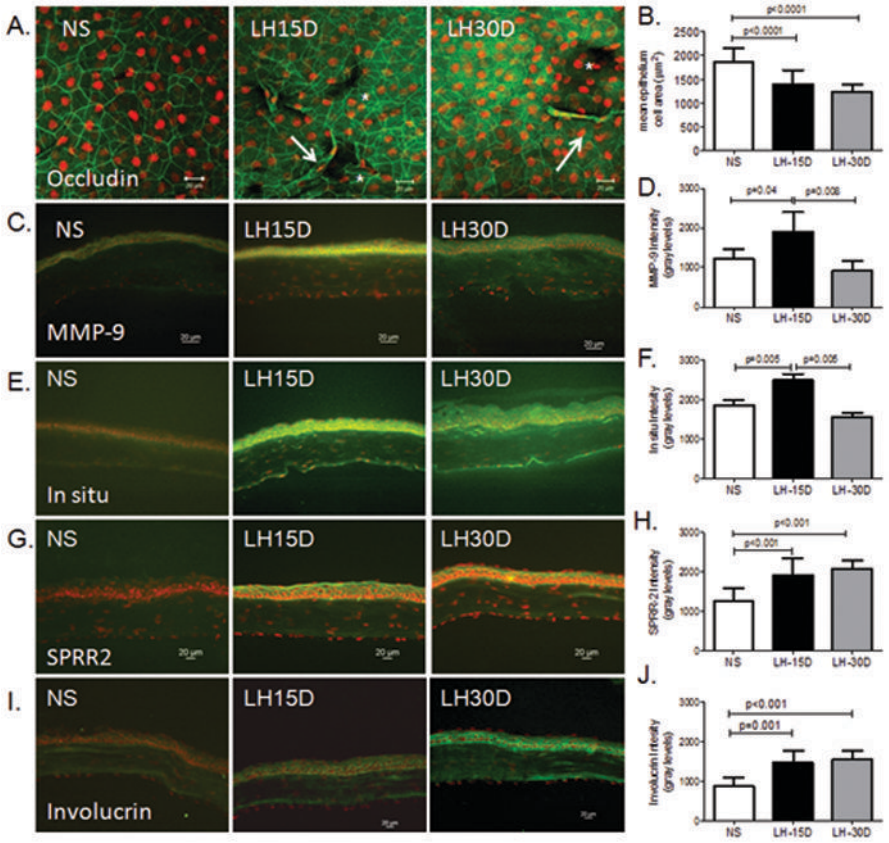

Figure 3. Expression of MMP-9 and cornified envelope precurssors

A. Representative merged digital images of laser scanning confocal microscopy images of whole mount corneas stained with polyclonal occludin antisera (in green) with propidium iodide (PI counterstaining (red) showing apical corneal epithelium of all experimental groups (nonstressed control (NS), low humidity stress (LH15D, and LH30D)). Asterisks indicate holes in the apical cell layer and arrows indicate detached cells.

B: Mean ± SD of epithelium cell area as measured as indicated in the Material and methods section.

C: Representative merged digital images of corneas cryosections immunostained for MMP-9.

D: Bar graphs of mean fluorescence intensity ± SD of MMP-9 immunostaining in corneal epithelium.

E: Representative digital images of in situ zymography used to generate intensity graph in F.

F: Graphical data are the mean ± SD of measured fluorescence levels of in situ assay in corneal epithelium. The fluorescence intensity is proportional to gelatinase activity, within the tissue

G: Representative merged digital images of corneas cryosections immunostained for small proline-rich protein-2, SPRR2

H: Bar graphs of mean fluorescence intensity ± SD of SPRR2 immunostaining in corneal epithelium immunostaining in corneal epithelium.

I: Representative merged digital images of corneas cryosections immunostained for involucrin

J: Bar graphs of mean fluorescence intensity ± SD of involucrin immunostaining in corneal epithelium.

Groups are: nonstressed control (NS), low humidity stress for 15 or 30 days (LH15D, and LH30D), all scale bars are 20 μm.

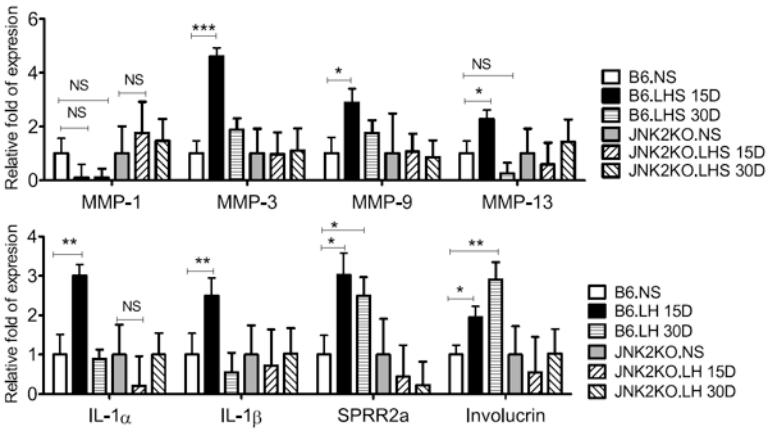

Figure 4. Gene expression analysis

Relative fold of expression showing mean ± SD (error bars) of matrix metalloproteinases (MMP)-1,-3, -9, -13, IL-1α, IL-1β, SPRR-2a and involucrin mRNA transcripts in cornea epithelia of nonstressed (NS) C57BL/6 (B6) and JNK2KO mice subjected to low humidity (LHS) stress at various time points (from 15 to 30 days). * P≤0.05;** P<0.001; *** P<0.001; NS=non-significant

Table 1

Oligonucleotide Primers Used for Real-Time PCR

Gene Name	Symbol	Assay ID*
Matrix metalloproteinase 1	MMP-1	Mm00473493_m1
Matrix metalloproteinase 3	MMP-3	Mm00440295_m1
Matrix metalloproteinase 9	MMP-9	Mm00442991_m1
Matrix metalloproteinase 13	MMP-13	Mm00439491_m1
Interleukin 1 alpha	IL1-α	Mm00439620_m1
Interleukin 1 beta	IL1-β	Mm00434228_m1
Involucrin	Involucrin	Mm00515219_s1
Small proline-rich 2	Sprr2a	Mm00845122_s1

*Identification number from Applied Byosistems (www.appliedbiosystems.com).